

## USING HYPERSPECTRAL DATA FOR MONITORING AND OBSERVATION OF FABA BEAN CROP GROWTH

Tarek FOUDA, Abeer ABDELSALAM

Tanta University, Faculty of Agriculture, Agriculture Engineering Department, Egypt, Emails:  
tfouda628@gmail.com, abeergmail1369@gmail.com

**Corresponding author:** tfouda628@gmail.com

### Abstract

*The optical imagery at high spatial resolution to monitoring and observation of faba bean crop growth obtained from The Sentinel-2 sensor during November 2021 to February 2022 (daytime) were used. Thirteen bands of multispectral data covering the visible, near-infrared, and short wave infrared portions of the spectrum using to monitor land cover change for environmental monitoring. A surface emissivity calculation is the first step of land surface temperature observation and finding the agricultural indices of faba bean crop. The emissivity per pixel was obtained directly from Sentinel-2 sensor data. Natural surfaces at the resolution of 30 m are heterogeneous and they differ from each other in their emissivity. In the present study, surface emissivity was evaluated by analysis of NDVI, NDMI, SWIR, NDWI, Agriculture Composite, and SAVI of vegetation cover per pixel, and the maximum values of climatic indices such as sunshine duration, relative humidity, long, short wave radiation, ultraviolet radiation direct, diffuse radiation, soil temperature, FAO reference evapotranspiration (E<sub>o</sub>). The results showed the monthly composite pictures which produced using to generate correct crop growth findings by comparing band reflectance values, vegetation indices, and environmental indicators.*

**Key words:** Faba bean, Sentinel-2, Monitoring, NDVI, NDMI, SWIR, NDWI

### INTRODUCTION

Faba bean (*Vicia faba* L.) was one of the first crops cultivated around 10,000 years ago. It is cultivated on every inhabited continent, with around 4 million tonnes produced per year. Of the starch-containing legumes, it has the greatest protein content, with a global average of 29% dry matter and a global average yield of 2.0 t/ha, indicating a high potential protein output per hectare in favourable conditions [1].

In the Mediterranean Basin, faba beans are often seeded in October to take advantage of the rainy winter months [9].

Its cultivation throughout the globe has undergone a fall since the middle of the twentieth century, with the area declining from more than 830,000 hectares in the early 1960s to only 109,000 ha in 2021 [3].

*Vicia faba* L. is a multi-purpose crop that is highly appreciated throughout North and East Africa; yet, output is still below demand, and productivity is low in many countries. This is mostly due to several issues, including the prevalence of low-yielding cultivars, a poor

seed system in many areas, vulnerability to abiotic and biotic challenges, a lack of better cultivars, and a lack of expansion [2].

Furthermore, it ranks top among the cold season food legumes produced in North and East Africa, with output averaging 1.6 and 0.7 million tonnes collected from 0.76 and 0.07 million hectares for dry and green faba beans, respectively [5].

Faba bean green pods and grains are gaining popularity in North African countries such as Egypt (190,937 tonnes), in addition to their traditional use as dry seeds (39,629 tonnes) [12].

Satellite remote sensing has already helped researchers improve and map minerals, rock kinds, crop growth, and other geological and agricultural properties. Since the introduction of Landsat-1 in 1972, the use of satellite pictures for agricultural research, particularly mapping agricultural units, has progressed significantly and successfully by employing multispectral data from the Advanced Space borne Thermal Emission and Reflection Radiometer Sentinel-2 [8].

Image processing technologies was utilized to automatically evaluate the size and shape of faba bean during growth periods. Shape measurement methods are mostly based on these models and are necessary for an accurate description, enabling comparison between polymorphisms or developmental periods [6].

Different ways that combine these methodologies with machine learning techniques have also been presented for observing agricultural growth. Spectral indices are only used to extract vegetation characteristics if the approaches are simple and effective enough. These include the false color composite index, normalized difference vegetation index (NDVI), enhanced vegetation index (EVI), barren soil visualization index, moisture stress NDMI, agriculture composite index, and normalized difference moisture index (NDMI) [13].

To develop reliable crop classification maps, multitemporal techniques must be used, as cultivations vary their spectral and textural appearance depending on the crop type growth cycle. Sentinel 2 data, which provides dense Time Series (TSs) of multispectral pictures with great spatial resolution, is a valuable information source [11].

The utilization of multi-temporal remote sensing data for enhanced spectral feature recognition and change detection is critical to crop-growth mapping, and optical Sentinel-2 multi-temporal imaging gives more accurate information and an improvement in classification accuracy in this way [7].

Temperature, sunshine duration, solar radiation, longwave radiation, UV radiation, direct radiation, diffuse radiation, soil temperature, and evapotranspiration are some of the climatic factors that affect faba bean cultivation.

Temperature influences the germination, growth, flowering, and pod formation of beans.

The optimal temperature range for beans is 15-25°C.

Sunshine duration and solar radiation determine the amount of photosynthesis and biomass production of fab beans.

The optimal sunshine duration for beans is 8-10 hours per day. Solar radiation consists of different components, such as direct radiation from the sun, diffuse radiation from the sky, and longwave radiation from the atmosphere. Direct radiation is more intense and beneficial for beans than diffuse radiation, but it can also cause heat stress and water loss. Diffuse radiation can penetrate deeper into the canopy and enhance the photosynthesis of lower leaves. Longwave radiation is the main source of heat loss for faba beans at night. UV radiation can damage the DNA and proteins of beans, reducing their yield and quality. Soil temperature affects the root growth and nutrient uptake of beans. The optimal soil temperature for beans is 16-24°C. Evapotranspiration is the combined loss of water from the soil and the plant surface. It influences the water balance and irrigation requirements of faba bean. The optimal evapotranspiration rate for beans is 4-6 mm/day [15].

The objective of this study was the possibility of using the satellite images to monitoring and observation of faba bean crop growth starting from agriculture to harvesting and measuring agricultural and climatic indicators during that period based multispectral imager bands of sentinel-2.

## MATERIALS AND METHODS

A field experiment was conducted to grow faba bean in the village of KafrEssam - Gharbia - Egypt, studying the vegetative and environmental indicators from planting in November 2021 until harvesting in February 2022, and monitoring and analysing developments in the Department of Agricultural Engineering - Faculty of Agriculture - Tanta University. As shown in Photo 1 and scientific classification of faba bean crops was shown in Table 1.



Photo 1. Faba bean crops  
 Source: Authors' determination.

Table 1. Scientific Classification of Faba Bean Crops

Kingdom	Plantae
Family	Fabaceae
Genus	Vicia
Order	Fabales
Tribe	Fabeae
Subfamily	Faboideae

Source: Wikipedia, Viciafaba,  
[https://en.wikipedia.org/wiki/Vicia\\_faba](https://en.wikipedia.org/wiki/Vicia_faba) [14].

### Satellite Data

is an Earth observation mission from the Copernicus and sentinel hub (EO)programme that provides high-resolution images in the visible and infrared wavelengths, to monitor vegetation, soil and water cover, and inland waterways as shown in Photo 2 and the specification of the satellite was shown in Table 2. Also, the Spatial resolutions were 10m, 20m, and 60m, depending on the wavelength as shown in Table 3.



Photo 2. Model of a Sentinel-2 satellite  
 Source: <https://earth.esa.int/web/sentinel/technical> [4].

Table 2. Specification of Sentinel-2 satellite

<b>Manufacturer</b>	<b>Astrium/Airbus</b>
	Thales Alenia Space
	Boostec
	Jena-Optronik
<b>Operator</b>	European Space Agency
<b>Applications</b>	Land and sea monitoring, natural disasters mapping, sea ice observations, ships detection

Source: <https://earth.esa.int/web/sentinel/technical> [4].

Table 3. Spectral bands for the SENTINEL-2 sensors

Sentinel-2 bands	Central wavelength, $\mu\text{m}$	Resolution, m
<b>Band 1-coastal aerosol</b>	0.443	60
<b>Band 2-blue</b>	0.490	10
<b>Band 3-green</b>	0.560	10
<b>Band 4-red</b>	0.665	10
<b>Band 5-vegetation red edge</b>	0.705	20
<b>Band 6- vegetation red edge</b>	0.740	20
<b>Band 7- vegetation red edge</b>	0.783	20
<b>Band 8-NIR</b>	0.842	10
<b>Band 8A- vegetation red edge</b>	0.865	20
<b>Band 9-water vapour</b>	0.945	60
<b>Band 10-SWRI-cirrus</b>	1.375	60
<b>Band 11- SWRI</b>	1.610	20
<b>Band 12- SWRI</b>	2.190	20

Source: <https://www.numerade.com> [10].

### Copernicus browser

The Copernicus program is a European Union initiative that aims to provide reliable and up-to-date Earth observation data for a variety of applications, including environmental monitoring, and climate change analysis. The Sentinel satellites are a key component of the Copernicus program, providing high-quality and frequent Earth observation data as shown in Photo 3.

### Sentinel hub browser

Sentinel Hub is a platform that provides access to Earth observation (EO) data, specifically satellite imagery. Sentinel Hub is known for its integration with the European Space Agency's (ESA) Copernicus program, which includes the Sentinel satellites.

Sentinel Hub simplifies the process of accessing and analysing satellite imagery by

offering a cloud-based infrastructure and an application programming interface (API) as shown in Photo 4.

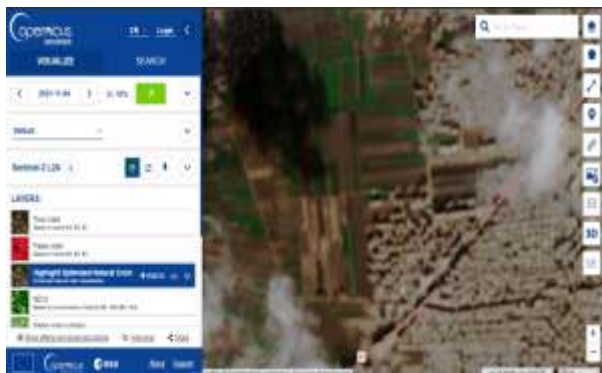


Photo 3. Copernicus browser interface  
 Source: Authors' determination.

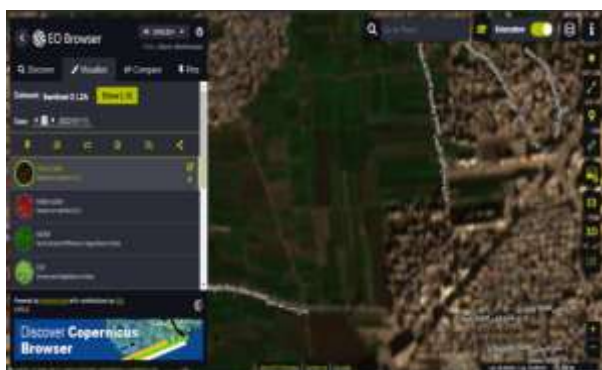


Photo 4. Sentinel hub browser interface  
 Source: Authors' determination.

### Experimental Field

The experimental field was located in KafrEssam, Tanta Governorate. between 30°48'15.9"N 30°58'56.2"E. The experimental field was plowed to a depth of 15 cm and leveled by a leveler machine. Also, the experimental field was irrigated abundantly once before planting for weed resistance. Also, after planting, the crop was fertilized using 45 kg of ammonium sulphate + 2 kg of potassium sulphate + 35 kg of superphosphate. Two weeks after planting, the crop was sprayed with 60 g of iron - 60 g of zinc - 60 g of manganese - 0.2 g of iron - 60 g of copper - 2 kg of urea. Photo 5 shows the true color of the farmland (based on B4, B3, and B2) before planting faba bean seeds.

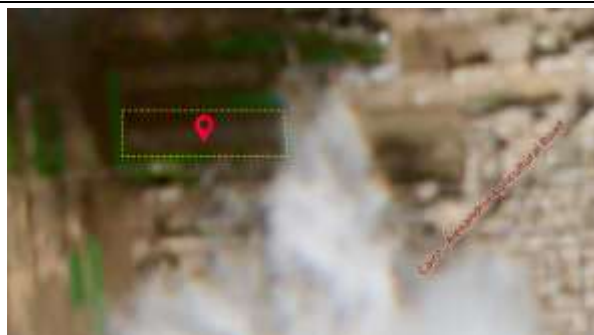


Photo 5. Farmland by SENTINEL-2  
 Source: Authors' determination.

### -Visualization Of Agricultural Indices False Color Composite Index

A false color composite based on B8, B4, and B3 uses at least one non-visible wavelength to image Earth. The false color composite using near-infrared, red, and green bands is very popular (a band is a region of the electromagnetic spectrum; a satellite sensor can image Earth in different bands). The false color composite is most commonly used to assess plant density and health, since plants reflect near infrared and green light, while they absorb red. Cities and exposed ground are grey or tan, and water appears blue or black.

### Normalized Difference Vegetation Index (NDVI)

NDVI built on a combination of bands (B8 and B4) is a simple, but effective index for quantifying green vegetation. It is a measure of the state of vegetation health based on how plants reflect light at certain wavelengths. The NDVI has a value range of -1 to 1. Water is represented by NDVI values that are negative (numbers that are close to -1). Arid patches of rock, sand, or snow are typically represented by values near zero (-0.1 to 0.1). Shrub and grassland are represented by low, positive values (between 0.2 and 0.4), while temperate and tropical rainforests are represented by high values (values close to 1) as shown in Photo 6.

$$NDVI = \frac{B8 - B4}{B8 + B4} \dots \dots \dots (1)$$

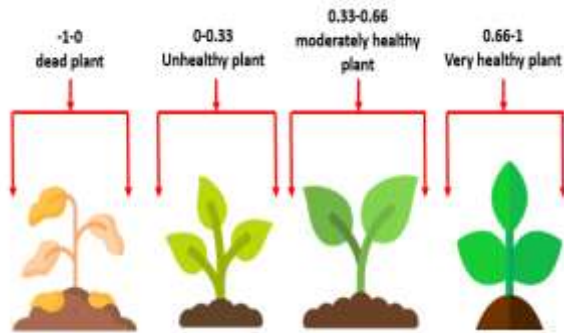


Photo 6. Normalized Difference Vegetation Index of plants  
 Source: Authors' drawing.

**Normalized Difference Moisture Index (NDMI)**

The normalized difference moisture Index (NDMI) based on (B8 and B11) is used to determine vegetation water content and monitor droughts. The value range of the NDMI is -1 to 1. Negative values of NDMI (values approaching -1) correspond to barren soil. Values around zero (-0.2 to 0.4) generally correspond to water stress. High, positive values represent high canopy without water stress (approximately 0.4 to 1).

$$NDMI = \frac{B8 - B11}{B8 + B11} \dots \dots \dots (2)$$

**Short Wave Infrared Composite (SWIR).**

Short wave infrared (SWIR) measurements (based on bands B12, B8A, B4) can help estimate how much water is present in plants and soil, as water absorbs SWIR wavelengths.

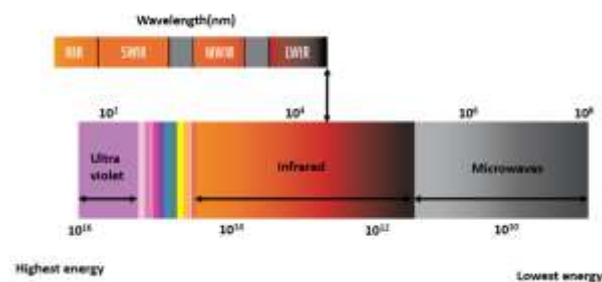


Photo 7. Electromagnetic Spectrum Illustrating SWIR Wavelength Range  
 Source: Authors' drawing.

Short wave infrared bands (a band is a region of the electromagnetic spectrum) are also useful for distinguishing between cloud types (water clouds versus ice clouds), snow, and

ice, all of which appear white in visible light. In this composite vegetation appears in shades of green, soils and built-up areas are in various shades of brown, and water appears black as shown in Photo 7.

**Normalized Difference Water Index (NDWI)**

NDWI Index based on a combination of bands (B3 and B8) is a remote sensing index that is commonly used to identify the presence of water in various environments and is particularly useful for distinguishing between water bodies and other land cover types. It is based on the fact that water absorbs light in certain spectral bands, leading to differences in reflectance values.

$$NDWI = \frac{B3 - B8}{B3 + B8} \dots \dots \dots (3)$$

**Agriculture Composite**

This composite based on bands B11, B8, B2 uses short-wave infrared, near-infrared and blue bands to monitor crop health (a band is a region of the electromagnetic spectrum). Both short-wave and near infrared bands are particularly good at highlighting dense vegetation, which appears dark green in the composite. Crops appear in a vibrant green and bare earth appears magenta.

**Soil Adjusted Vegetation Index (SAVI).**

The soil adjusted vegetation index is similar to (NDVI) but is used in areas where vegetative cover is low (< 40%). The index is a transformation technique that minimizes soil brightness influences from spectral vegetation indices involving red and near-infrared (NIR) wavelengths. The index is helpful when analysing young crops, arid regions with sparse vegetation and exposed soil surfaces.

$$SAVI = \frac{B8 - B4}{B8 + B4 + L} \times (1 + L) \dots \dots \dots (4)$$

where:

L is the soil brightness correction factor and could range from (0 -1).

**-Climatic And Environmental Indices.**

**Sunshine Duration**

Sunshine duration, which is usually expressed in hours per day, is the length of time that the sun is visible or the amount of sunshine that occurs over a given period of time. The

following formula can be used to determine the length of sunshine, and it is based on the ratio of the actual length of sunshine to the maximum length of sunshine that can occur in a given period:

$$SD = \frac{\text{Actual Sunshine Duration}}{\text{Maximum Possible Sunshine Duration}} \times 24, \text{min} \dots\dots\dots(5)$$

**Relative Humidity**

Relative Humidity (RH) is a measure of the amount of moisture present in the air compared to the maximum amount of moisture the air can hold at a specific temperature. It is expressed as a percentage and indicates how close the air is to being saturated with moisture, and is given by the following formula:

$$RH = \frac{\text{Actual Water Vapor Pressure}}{\text{Saturated Water Vapor Pressure at the Same Temperature}} \times 100(6)$$

**Longwave Radiation**

Terrestrial, thermal, and infrared radiation are other names for long wave radiation. It is electromagnetic radiation that falls between about 3 and 100 mm in the spectral band. This range of emissions is produced by Earth surface temperatures, with the highest terrestrial radiation occurring at a wavelength of roughly 10 mm. Spectrally combined longwave radiation can be estimated from the Stefan-Boltzmann equation:

$$Q = \epsilon \sigma A T^4 \dots\dots\dots(7)$$

where:

Q is the longwave radiation (in watts) emitted by the surface, W/m<sup>2</sup>

ε is the emissivity of the surface, which ranges from 0 to 1 and represents the efficiency of the surface in emitting radiation.

σ is the Stefan-Boltzmann constant (5.67×10<sup>-8</sup> W m<sup>-2</sup>K<sup>-4</sup>).

A is the surface area of the emitting body, m<sup>2</sup>

T is the absolute temperature of the emitting body in Kelvin.

**Ultraviolet Radiation, W/m<sup>2</sup>**

UV radiation is a form of electromagnetic radiation with shorter wavelengths than visible light but longer wavelengths than X-rays. It is invisible to the human eye.

**Direct Radiation, W/m<sup>2</sup>**

The solar radiation that travels in a straight line from the Sun to the Earth's surface is referred to as direct radiation, sometimes known as direct sunlight or direct solar radiation. It is the portion of solar radiation that passes through the atmosphere of Earth directly without being absorbed or scattered by particles, water vapor, or other gases in the atmosphere.

$$P = A G \cos \theta, \text{ W/m}^2 \dots\dots\dots(8)$$

where:

A is the surface area perpendicular to the sun's rays, m<sup>2</sup>

G is the solar constant (approximately 1361 W/m<sup>2</sup>)

θ is the angle of incidence of the sun's rays on the surface.

**Diffuse Radiation, W/m<sup>2</sup>**

Diffuse radiation refers to solar radiation that reaches the Earth's surface after being scattered or reflected by the atmosphere.

$$D = K_d \times I_{\text{extraterrestrial}}, \text{ W/m}^2 \dots\dots\dots(9)$$

where:

K<sub>d</sub> is the diffuse fraction, representing the ratio of diffuse radiation to extra-terrestrial radiation,

I<sub>extra-terrestrial</sub> is the extra-terrestrial solar radiation on a horizontal surface (in W/m<sup>2</sup>).

**Soil Temperature, °C**

Soil temperature refers to the measure of the thermal energy present in the soil. It is an important parameter that influences various soil processes, and plant growth activity.

**FAO Reference Evapotranspiration (ET<sub>o</sub>)**

Evapotranspiration is a combined process involving the evaporation of water from surfaces and the transpiration of water from plants.

$$ET_o = \frac{0.408 \Delta (R_n - G) + \gamma \left( \frac{900}{T+273} \right) u_2 (e_s - e_a)}{\Delta + \gamma (1 + 0.34 u_2)}, \text{ mm} \dots\dots\dots(10)$$

where:

R<sub>n</sub> the net radiation at the crop, MJ m<sup>-2</sup> day<sup>-1</sup>

G is the soil heat flux density, MJ m<sup>-2</sup> day<sup>-1</sup>

Δ the slope of the saturation vapour pressure curve, KPa/°C,

γ the psychrometric constant, KPa/°C,

T is the mean daily air temperature at 2 meters above the ground, °C

u<sub>2</sub> is the wind speed at 2 meters above the ground/s

e<sub>s</sub> is the saturation vapour pressure, KPa

e<sub>a</sub> is the actual vapour pressure, KPa

**Shortwave Radiation**

The term "shortwave radiation" describes the solar radiation that reaches Earth's surface. Shorter wavelength electromagnetic waves, such as visible light and some ultraviolet (UV) and infrared (IR) radiation, make up the majority of it.

Although the sun emits energy across a wide range, shortwave radiation makes up the majority of solar radiation that reaches Earth.

$$\text{Shortwave Radiation (SW)} = \text{Solar Constant} \times \text{Solar Declination} \times (\cos(\text{Latitude}) \times \cos(\text{Solar Hour Angle}) \times \sin(\text{Solar Elevation Angle})) + \frac{2\pi \times 10^{-7}}{8000} \times \text{Elevation}, \quad \text{W/m}^2 \quad (11)$$

**RESULTS AND DISCUSSIONS**

Data sets for the research region are provided for four time periods (November, December, January, and February) through season 2021-2022, processed to give resemble false-color infrared photography, with red indicating the presence of thick green vegetation, as shown in Photo 8. It also offers a clear indication and overview of the sorts of changes that have occurred throughout the region over the last many months (faba bean crop growth periods).

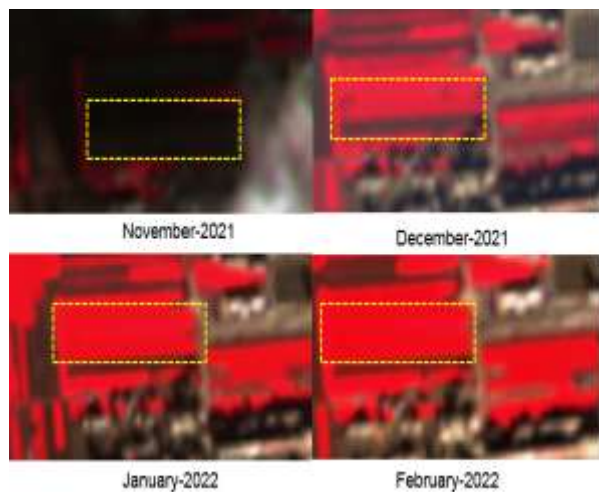


Photo 8. False color composite index during periods of crop growth  
 Source: Authors' determination.

The results show an increase in plant density from December to February, particularly in the box area of the picture, as shown by the degree of red (associated with the greenness of the flora) in the photos. By increasing vegetation cover, the NDVI values increased as shown in Photo 9.

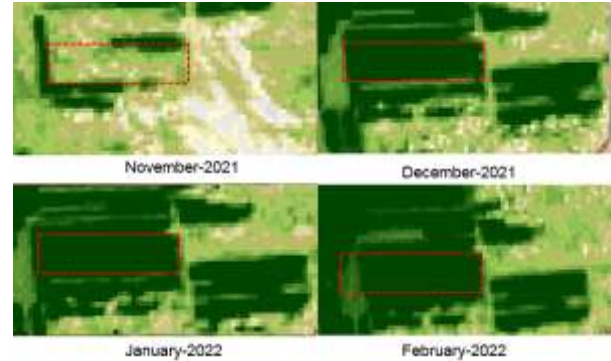


Photo 9. Normalized difference vegetation index during periods of crop growth  
 Source: Authors' determination.

Also, the frequency distribution curve shows the maximum values for growth periods were 0.052, 0.083, 0.12, and 0.03 as shown in Photo 10, and this means that NDVI values were decreased during the study time.

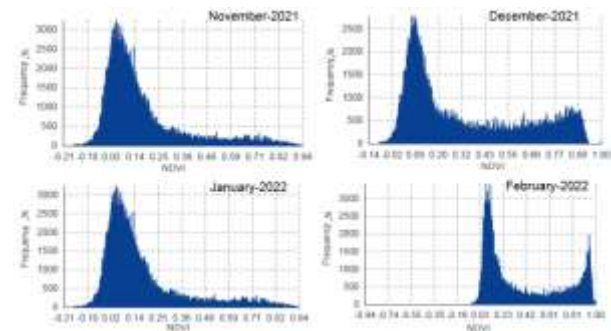


Photo 10. Frequency distribution of normalized difference vegetation index  
 Source: Authors' determination.

Photo 11 and Photo 12 show that the value of NDWI and NDMI has been observed, and direct correlations reveal that an increase or decrease in the value of NDVI corresponds to an increase or reduction in the value of NDMI and NDWI based on frequency distribution curve which shows the maximum values of NDMI and NDWI during growth periods were (-0.11, -0.27), (-0.07, -0.24), (-0.09, -0.91), and (-0.05, -0.22) respectively as shown in Photo 13 and Photo 14.

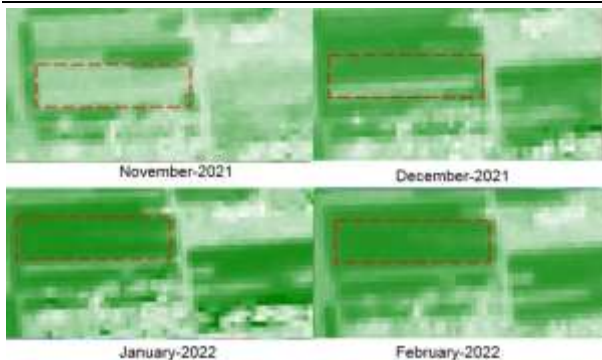


Photo 11. Normalized difference water index during periods of crop growth  
 Source: Authors' determination.

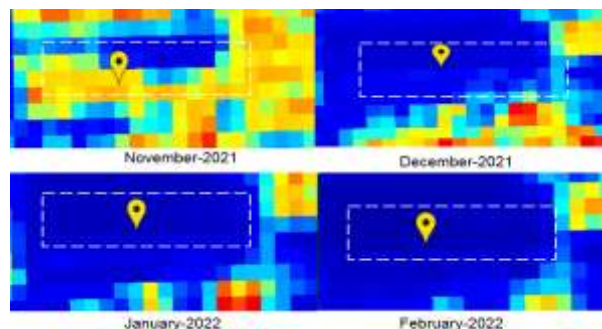


Photo 12. Normalized difference moisture index during periods of crop growth  
 Source: Authors' determination.

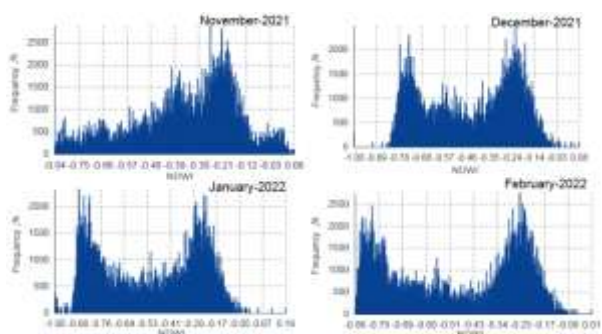


Photo 13. Frequency distribution of normalized difference water index  
 Source: Authors' determination.

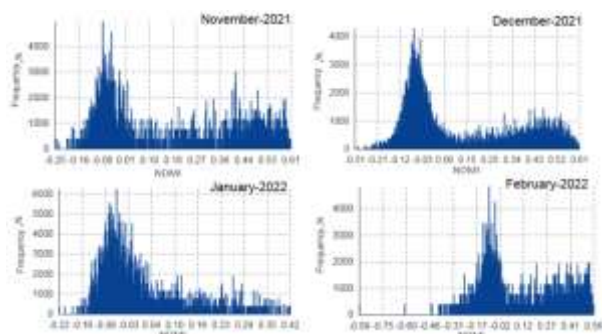


Photo 14. Frequency distribution of normalized difference moisture index  
 Source: Authors' determination.

The results of the SWIR and agriculture

composite index show an increase in plant density during the crop growth periods until harvest, especially in January and February 2022 as shown in Photo 15 and Photo 16.

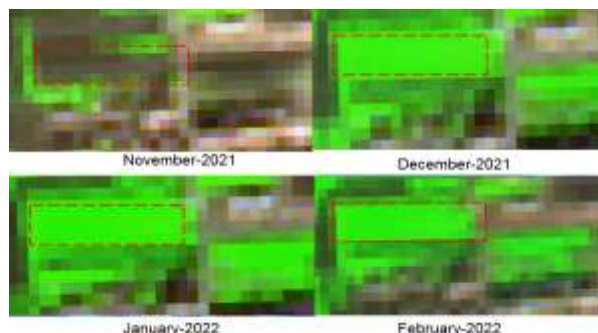


Photo 15. Short wave infrared composite during periods of crop growth  
 Source: Authors' determination.

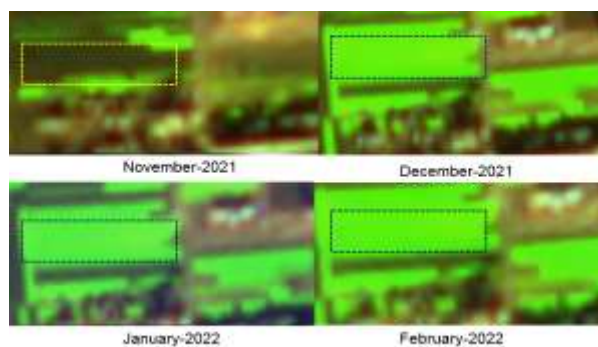


Photo 16. Agriculture composite during periods of crop growth  
 Source: Authors' determination.

The results show an increase in the SAVI during the crop growth period based on NDVI results as shown in Photo 17, and the frequency distribution curve shows the maximum values during growth periods were 0.015, 0.043, 0.055, and 0.011 as shown in Photo 18.

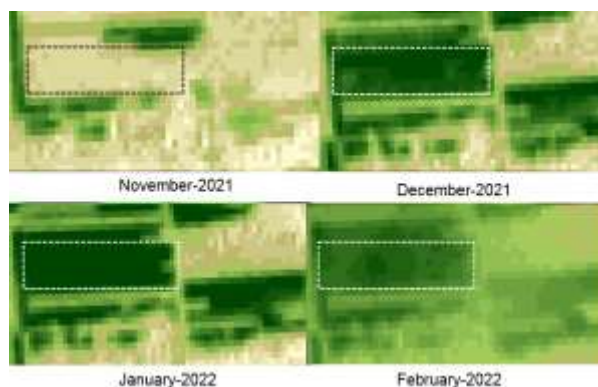


Photo 17. Soil adjusted vegetation index during periods of crop growth  
 Source: Authors' determination.



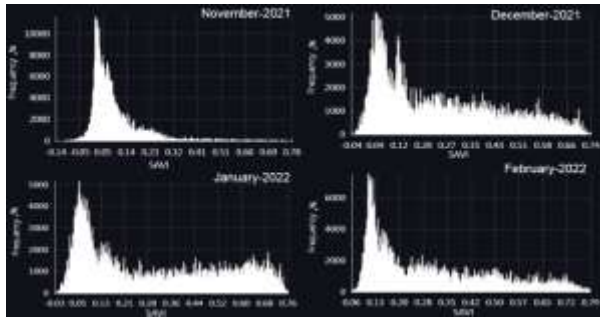


Photo 18. Frequency distribution of soil adjusted vegetation index  
 Source: Authors' determination.

### Climatic and environmental indices

Fig. 1 showed the maximum and the minimum values of direct and diffuse short wave radiation were (56.69, and 34.67), and (13.74, and 17.32  $W/m^2$ ) in February 2022 and December 2021 respectively. In January 2022, the minimum values of sunshine duration and uv radiation were (5.14, and 4.66  $W/m^2$ ), and the maximum values of same indices were (13.99, and 9.34  $W/m^2$ ) in February 2022 respectively as shown in Fig. 2. The results of evapotranspiration and FAO reference evapotranspiration as shown in Fig. 3, the maximum values were (0.043, and 0.047 mm) in November 2021, February 2022. Also, the minimum values were (0.30, 0.022 mm) in February 2022 and December 2021 respectively. The maximum and minimum values of temperature and soil temperature during growth periods of faba bean crop were (7.64, 10.83), and (4.41, 3.70 $^{\circ}C$ ) respectively as shown in Fig. 4.

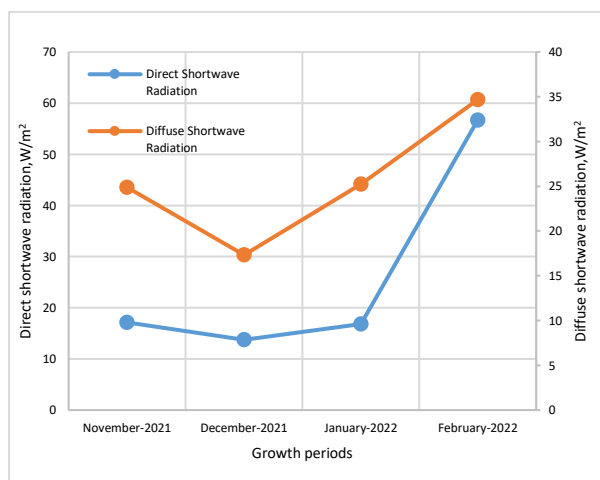


Fig. 1. Relationship between direct and diffuse short wave radiation during periods of crop growth  
 Source: Authors' determination.

Therefore, the previous results show an expulsion relationship between the indicators. Fig. 5 and Fig. 6 showed the results of relative humidity, short and long wave radiation were (84.91.36%, and 304.33  $W/m^2$ ) as a maximum values, when the minimum values of the same indices were (79.03%, 31.07, and 272.21  $W/m^2$ ) during growth periods.

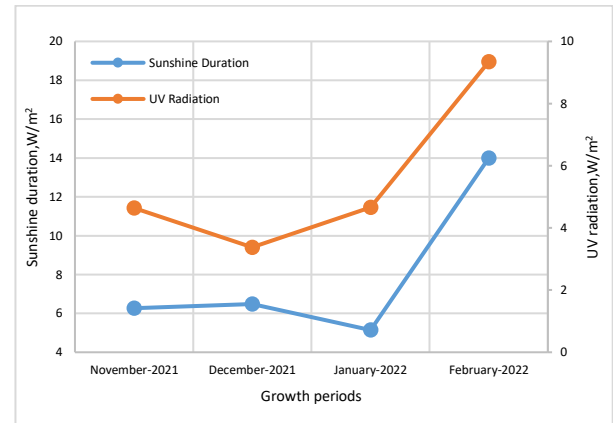


Fig. 2. Relationship between sunshine duration and uv radiation during periods of crop growth  
 Source: Authors' determination.

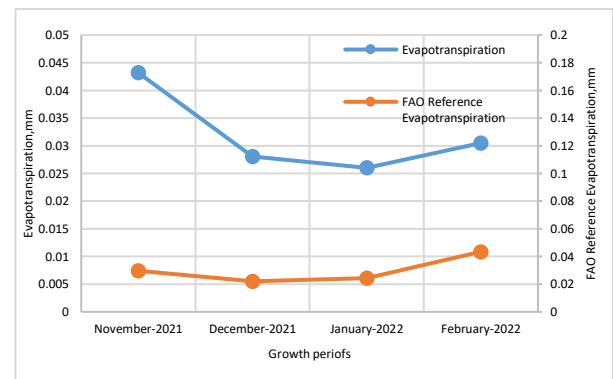


Fig. 3. Relationship between evapotranspiration and FAO reference evapotranspiration during periods of crop growth  
 Source: Authors' determination.

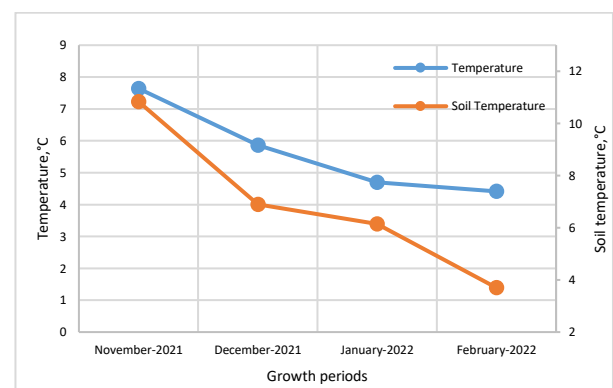


Fig. 4. Relationship between temperature and soil temperature during periods of crop growth  
 Source: Authors' determination.

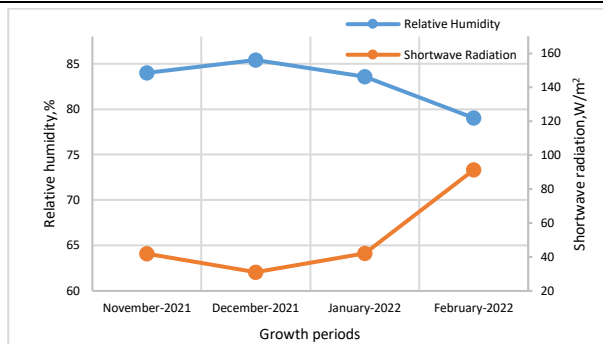


Fig. 5. Relationship between relative humidity and short wave radiation during periods of crop growth  
 Source: Authors' determination.

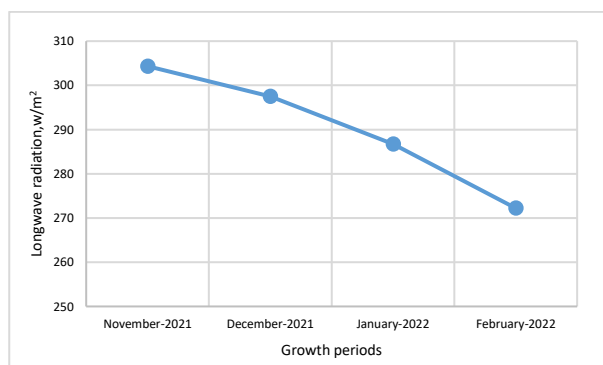


Fig. 6. Relationship between long wave radiation and periods of crop growth  
 Source: Authors' determination.

## CONCLUSIONS

Hyperspectral imaging become a popular research tool that facilitates thorough non-destructive analyses by simultaneous acquisition of both spectral and spatial information of agricultural samples. It can be used as an emerging technology for monitoring quality parameters in field crops. The open-access remote-sensing datasets and the processing capacity of the EO platform were critical to realizing the goals of this research. In this study It is possible to use hyperspectral reflectance data extracted monthly from composite pictures were produced using Sentinel-2 to monitor and observation of faba bean crop growth which evaluated by analysis of NDVI, NDMI, SWIR, NDWI, Agriculture Composite, and SAVI of vegetation cover per pixel, and the maximum values of climatic indices such as sunshine duration, relative humidity, long, short wave radiation, ultraviolet radiation direct, diffuse radiation, soil temperature,

FAO reference evapotranspiration (Eto) during faba bean growth period.

## REFERENCES

- [1] Abobatta, W.F., El-Hashash, E.F., Hegab, R.H., 2021, Challenges and opportunities for the global cultivation and adaptation of legumes. *J Appl Biotechnol Bioeng* 8(5): 160–172. Accessed on 22 January, 2024.
- [2] Abou-Khater, L., Maalouf, F., Rubiales, D., 2022, Status of faba bean (*Vicia faba* L.) in the Mediterranean and East African countries. In *Developing Climate Resilient Grain and Forage Legumes* (pp. 297-327). Singapore: Springer Nature Singapore. Accessed on 22 January, 2024.
- [3] Belachew, K., Soederholm-Emas, A., Topp, C.F.E., Watson, C.A., Stoddard, F. L., 2023, Management factors affecting faba bean yield. *Legume Perspectives*, (24), 15-17. Advance online publication. [https://www.legumesociety.org/wp-content/uploads/2024/01/legum\\_perspect\\_24.pdf](https://www.legumesociety.org/wp-content/uploads/2024/01/legum_perspect_24.pdf), Accessed on 22 January, 2024.
- [4] Earth on line, 2023, <https://earth.esa.int/web/sentinel/technical>, Accessed on 22/1/2024.
- [5] FAO STAT, 2023, Food and Agriculture Organization of the United Nations. [www.faostat.fao.org](http://www.faostat.fao.org) Accessed on 22 January, 2024.
- [6] Fouda, T., Abdelsalam, A., Swilam, A., Didamony, M.E., 2023, 3D printing technology as an effective solution to build faba bean seed meter plate with various materials, *Scientific Papers. Series "Management, Economic Engineering in Agriculture and rural development"*, Vol. 23(1), 223-240. [https://managementjournal.usamv.ro/pdf/vol.23\\_1/volume\\_23\\_1\\_2023.pdf](https://managementjournal.usamv.ro/pdf/vol.23_1/volume_23_1_2023.pdf), Accessed on 22 January, 2024.
- [7] Hernandez, I., Benevides, P., Costa, H., Caetano, M., 2020, Exploring Sentinel-2 for land cover and crop mapping in Portugal. *The International Archives of the Photogrammetry, Remote Sensing and Spatial Information Sciences*, 43, 83-89. Accessed on 22 January, 2024.
- [8] Karimzadeh, S., Tangestani, M. H., 2021, Evaluating the VNIR-SWIR datasets of WorldView-3 for lithological mapping of a metamorphic-igneous terrain using support vector machine algorithm; a case study of Central Iran. *Advances in Space Research*, 68(6), 2421-2440. Accessed on 22 January, 2024.
- [9] Khazaei, H., O'Sullivan, D. M., Stoddard, F. L., Adhikari, K. N., Paull, J. G., Schulman, A. H., ... & Vandenberg, A., 2021, Advances in faba bean genetic and genomic tools for crop improvement. *Legume Science*, 3(3), e75. Accessed on 22 January, 2024.
- [10] Numerade.com, <https://www.numerade.com>. Accessed on 22 January, 2024.
- [11] Paris, C., Weikmann, G., Bruzzone, L., 2020, Monitoring of agricultural areas by using Sentinel 2 image time series and deep learning techniques.

In Image and Signal Processing for Remote Sensing XXVI (Vol. 11533, pp. 122-131). Accessed on 22/1/2024.

[12]Rahate, K. A., Madhumita, M., Prabhakar, P. K., 2021, Nutritional composition, anti-nutritional factors, pretreatments-cum-processing impact and food formulation potential of faba bean (*Vicia faba* L.): A comprehensive review. Lwt, 138, 110796, Accessed on 22 January, 2024.

[13]Sathianarayanan, M., Saraswat, A., Athick, A. M. A., Lin, H. M., 2023, Intercomparison between sentinel-1, sentinel-2, and landsat-8 on reservoir water level estimation. Sustainable Water Resources Management, 9(6), 185 Accessed on 22 January, 2024.

[14]Wikipedia, *Vicia faba*, [https://en.wikipedia.org/wiki/Vicia\\_faba](https://en.wikipedia.org/wiki/Vicia_faba), Accessed on 22/1/2024.

[15]Wydra, K., Vollmer, V., Busch, C., Prichta, S., 2023, Agrivoltaic: Solar Radiation for Clean Energy and Sustainable Agriculture with Positive Impact on Nature. Accessed on 22 January, 2024.

